

Coherent and Differential ICI Cancellation for Mobile OFDM with Application to DVB-H

Sili Lu, *Student Member, IEEE* and Naofal Al-Dhahir, *Fellow, IEEE*

Abstract—We develop a reduced-complexity hybrid frequency/time-domain orthogonal frequency division multiplexing (OFDM) channel estimation algorithm for high-mobility scenarios where the channel varies significantly within each OFDM block, resulting in severe intercarrier interference (ICI). The algorithm exploits the banded and symmetric structure of the channel matrix in the frequency-domain and its sparse structure in the time-domain to achieve significant complexity reductions, which we quantify for the Digital Video Broadcasting-Handheld (DVB-H) system. Furthermore, we compare coherent and differential mobile OFDM detection for DVB-H.

Index Terms—ICI mitigation, OFDM, channel estimation, doppler shift

I. INTRODUCTION

SUPPORTING high mobility is a key requirement for a number of OFDM-based broadband wireless systems, such as DVB-H[1]. For high-mobility systems, the fast channel variations within one OFDM block destroy the orthogonality between subcarriers resulting in ICI proportional to the Doppler frequency. This problem is even more severe for the DVB-H 8K mode (which uses a large number of 8192 densely-spaced subcarriers) and becomes a significant challenge for receiver reliability at highway and train speeds.

To mitigate ICI, several techniques have been proposed in the literature including linear minimum mean square error (MMSE) equalizers [2] [3], successive interference cancellation [4], basis expansion models (BEM) [5] and time-domain block filtering [6]. Our objective in this paper is to investigate low-complexity schemes that can suppress ICI effectively under high-mobility conditions. As a case study, we focus on the challenging DVB-H application where the number of subcarriers is very large (2048, 4096, or 8192) [7], hence it is critical to develop a low-complexity ICI cancellation solution due to the power/size constraints at the user terminal. One such scheme is the finite impulse response (FIR) MMSE frequency-domain equalizer (FEQ) in [8] which is based on the well-known banded structure of the channel matrix in the frequency-domain [9][10], and has only few taps per subcarrier. Nevertheless, all of these approaches are coherent detection schemes that require reliable channel estimation at the receiver which is a challenging task at high mobility.

Channel estimation for OFDM can be performed in the frequency domain or time domain. Conventional frequency-domain channel estimation algorithms ignore ICI which makes

them highly suboptimal under high Doppler. Time-domain channel estimation algorithms (such as [6]) typically mark a few rows of the time-domain channel matrix and estimate them using pilot tones embedded within each OFDM block. Since the multipath delay spread can be very high for single frequency network (SFN) DVB systems [1] [7], the number of unknown channel taps for each marker row can be too high to estimate with the limited number of available pilots. Considering a fast-varying channel, Mostofi *et al.* proposed in [11] a hybrid frequency/time-domain channel estimation algorithm based on a *linear* approximation of the channel time variations within one OFDM block.

As a low-complexity alternative transceiver structure, we also investigate and compare the performance of differential OFDM detection with coherent OFDM detection for the DVB-H system. Note that differential detection is already used in the digital audio broadcasting (DAB) standard. Since differential detection does not require channel estimation, pilot overhead can be reduced to increase data throughput and channel estimation complexity can be eliminated from the user terminal.

Our main contributions in this paper can be summarized as follows

- We show how to significantly reduce the complexity of the hybrid frequency/time-domain channel estimation algorithm in [11] by exploiting the channel's sparse and banded structure. We quantify these complexity savings through a detailed complexity analysis for the DVB-H system.
- We derive a new asymptotic relationship between the sub- and super-diagonals of the frequency-domain channel matrix and exploit it to further reduce the complexity of channel estimation and to design an ICI-mitigating pilot/data placement scheme.
- We investigate differential OFDM detection in the presence of ICI and compare its performance with coherent detection for the DVB-H system.

Notation: We use $(\cdot)^T$ to denote the transpose, $(\cdot)^*$ the complex-conjugate, $(\cdot)^H$ the complex-conjugate transpose, $\lfloor \cdot \rfloor$ the floor operation and $(\cdot)_N$ the modulo- N operation. $G_{i,j}$ denotes the element in the i -th row and j -th column of matrix \mathbf{G} , where row/column indices begin with zero. The estimated value of random variable a is denoted by \hat{a} and \mathbf{I}_N denotes the $N \times N$ identity matrix. We use the notation of $\mathbf{G}(:, j)$ to denote the j -th column of \mathbf{G} .

II. MOBILE OFDM SYSTEM MODEL

We consider an OFDM system with N subcarriers where each OFDM block, denoted by $\mathbf{X} = [X_0 \dots X_{N-1}]^T$, is converted into time-domain samples $\mathbf{x} = [x_0 \dots x_{N-1}]^T$ using the N -point Inverse Fast Fourier Transform (IFFT) operation $\mathbf{x} = \mathbf{F}^H \mathbf{X}$ where \mathbf{F}^H is the N -point IFFT matrix. We assume

Manuscript received June 4, 2007; revised September 17, 2007, November 8 2007 and November 25, 2007; accepted December 3, 2007. The associate editor coordinating the review of this letter and approving it for publication was Dr. R. Mallik.

This work was supported in part by Semiconductor Research Corporation under contract No. 2005-HJ-1328 and by a gift from Texas Instruments Inc.

The authors are with University of Texas at Dallas, (e-mail: {sxl059000, aldahahir}@utdallas.edu)

Digital Object Identifier 10.1109/TWC.2008.070591.

that the cyclic prefix (CP) length is equal to or larger than the channel impulse response (CIR) memory denoted by L . Then, the received block $\mathbf{y} = [y_0 \dots y_{N-1}]^T$ after CP removal is given by

$$\mathbf{y} = \mathbf{H}\mathbf{x} + \mathbf{v} \quad (1)$$

where \mathbf{H} is an $N \times N$ time-domain channel matrix with elements $H_{n,l} = h_{n,(n-l)_N}$ where $h_{n,l}$ is the CIR at lag l for $0 \leq l \leq L-1$ and time instant n for $0 \leq n \leq N-1$, and \mathbf{v} is the time-domain noise vector with auto-correlation matrix $\sigma^2 \mathbf{I}_N$. Taking the FFT of (1), we obtain

$$\mathbf{Y} = \mathbf{F}\mathbf{y} = \mathbf{F}\mathbf{H}\mathbf{F}^H \mathbf{X} + \mathbf{F}\mathbf{v} = \mathbf{G}\mathbf{X} + \mathbf{V} \quad (2)$$

where $\mathbf{G} \triangleq \mathbf{F}\mathbf{H}\mathbf{F}^H$ is the frequency-domain channel matrix and \mathbf{V} is the frequency-domain noise vector. For a quasi-static fading channel, \mathbf{H} is a circulant matrix and hence transforms into a diagonal \mathbf{G} matrix in (2). In this case, the OFDM subcarriers are decoupled, and hence a one-tap FEQ is optimal. For example, with a linear Zero-forcing (ZF) FEQ, the data estimate for the k -th subcarrier \hat{X}_k is simply $\hat{X}_k = G_{k,k}^{-1} Y_k$. For the time-varying channel, however, \mathbf{H} is not circulant and hence \mathbf{G} is no longer diagonal. In this case, the input-output relation for the k -th subcarrier is given by

$$Y_k = G_{k,k} X_k + \sum_{n=0, n \neq k}^{N-1} G_{k,n} X_n + V_k \quad (3)$$

The first term on the right-hand side of (3) is the desired signal term while the second term is the ICI term which can be characterized by the normalized Doppler frequency $F_d = f_d T$ where f_d is the Doppler frequency and T is the time duration of the useful part of one OFDM block.

III. COHERENT ICI CANCELLATION

A. ICI Analysis

To better understand the structure of \mathbf{G} , we expand the relation $\mathbf{G} = \mathbf{F}\mathbf{H}\mathbf{F}^H$ in (2) and get

$$G_{k,n} = \frac{1}{N} \sum_{m=0}^{L-1} \sum_{r=0}^{N-1} h_{r,m} e^{\frac{j2\pi r(n-k)}{N}} e^{-\frac{j2\pi n m}{N}} \quad (4)$$

For a quasi-static channel where $h_{r,m} = h_{s,m}$ for $r \neq s$, $0 \leq m \leq L-1$, and $0 \leq r, s \leq N-1$, we have

$$G_{k,n} = \begin{cases} \sum_{m=0}^{L-1} h_m^{\text{avg}} e^{-\frac{j2\pi m k}{N}} & : k = n \\ 0 & : k \neq n \end{cases} \quad (5)$$

where $h_m^{\text{avg}} = \frac{1}{N} \sum_{r=0}^{N-1} h_{r,m}$ denotes the time-average of the m -th channel tap and in this case $h_m^{\text{avg}} = h_{r,m}, \forall 0 \leq r \leq N-1$. It is clear from (5) that \mathbf{G} is a diagonal matrix with elements equal to the channel frequency response.

Turning our attention to fast-varying channels, the CIR is no longer fixed within one OFDM block. In [3] and [11], a linear model for the time-domain channel variations was proposed. It is shown in [11] that for Doppler rates normalized to the subcarrier spacing of up to 20%, the channel time-variations can be approximated by a piece-wise linear model with a constant slope over each OFDM block. Let α_m denote

the slope of the m -th CIR tap, then the m -th CIR tap at instant r can be expressed as [11]

$$h_{r,m} = h_m^{\text{avg}} + \Delta h_{r,m}; \quad \Delta h_{r,m} = \left(r - \frac{N-1}{2}\right) \alpha_m \quad (6)$$

where $\Delta h_{r,m}$ denotes the time-variation term at the m -th tap for $0 \leq r \leq N-1, 0 \leq m \leq L-1$. Here, we used the fact that the average of each channel tap can be approximated by the middle point of the channel tap vector, i.e. $h_m^{\text{avg}} \approx h_{N/2-1,m}$ as proved in [11]. Combining (4) and (6), we arrive at (7) shown on top of next page.

Therefore, the time-average term h_m^{avg} corresponds only to the diagonal elements of \mathbf{G} while the time-variation term $\Delta h_{r,m}$ contributes to the off-diagonal elements giving rise to ICI.

It is a well-known fact that \mathbf{G} has most of its energy concentrated along its main diagonal and hence can be approximated as a *banded* matrix (see e.g. [9][10] and the references therein), which has non-zero elements only along $(2D+1)$ main diagonals and two $D \times D$ triangular matrices in the top-right and bottom-left corners. This banded structure implies that most of the ICI term energy in (3) results from the adjacent subcarriers. Based on this banded structure, we proposed in [8] an FIR FEQ designed using the MMSE criterion (hence the name FIR-MMSE FEQ) which is based only on the following $(2D+1) \times (4D+1)$ submatrix of \mathbf{G} .

$$\mathbf{G}_m = \begin{bmatrix} G_{(m-D)_N, (m-2D)_N} & \cdots & G_{(m-D)_N, (m+2D)_N} \\ \vdots & \vdots & \vdots \\ G_{m, (m-2D)_N} & \cdots & G_{m, (m+2D)_N} \\ \vdots & \vdots & \vdots \\ G_{(m+D)_N, (m-2D)_N} & \cdots & G_{(m+D)_N, (m+2D)_N} \end{bmatrix} \quad (8)$$

The Q -tap (where $Q = 2D+1$) FIR-MMSE FEQ is given by [8]

$$\mathbf{w}_m = \mathbf{g}_m^H (\mathbf{G}_m \mathbf{G}_m^H + \sigma^2 \mathbf{I}_Q)^{-1} \quad (9)$$

where $\mathbf{g}_m = \mathbf{G}_m(:, 2D+1)$ is the middle column of \mathbf{G}_m . Hence, the Q -tap FEQ output for the m -th subcarrier is $\hat{X}_m = \mathbf{w}_m \mathbf{Y}_m$ where $\mathbf{Y}_m = [Y_{(m-D)_N} \dots Y_{(m+D)_N}]^T$.

To compute the coefficients for this FIR-MMSE FEQ, we need to estimate the Q (typically $Q = 2D+1 = 3$) diagonals of \mathbf{G} . The hybrid frequency/time-domain channel estimation algorithm of the next subsection provides a computationally-efficient solution for this problem.

Starting from (7), we show in the Appendix that for large N , the elements of the sub-diagonals of \mathbf{G} are approximately the negatives of the corresponding elements of the super-diagonals, i.e. $G_{i+1,i} \approx -G_{i-1,i}$. We will utilize this property to simplify the channel estimation algorithm in Subsection III-B and develop an efficient ICI-mitigating pilot/data placement scheme in Subsection III-C.

B. Reduced-Complexity Hybrid Channel Estimation Algorithm

To estimate the Q main diagonals of \mathbf{G} , we revisit the hybrid frequency/time-domain channel estimation algorithm in [11]. Let $\mathbf{h}^{\text{avg}} = [h_0^{\text{avg}} \ h_1^{\text{avg}} \ \dots \ h_{L-1}^{\text{avg}}]$ and $\boldsymbol{\alpha} =$

$$\begin{aligned}
G_{k,n} &= \frac{1}{N} \sum_{m=0}^{L-1} \sum_{r=0}^{N-1} h_m^{\text{avg}} e^{\frac{j2\pi r(n-k)}{N}} e^{-\frac{j2\pi nm}{N}} + \frac{1}{N} \sum_{m=0}^{L-1} \sum_{r=0}^{N-1} \Delta h_{r,m} e^{\frac{j2\pi r(n-k)}{N}} e^{-\frac{j2\pi nm}{N}} \\
&= \begin{cases} \sum_{m=0}^{L-1} h_m^{\text{avg}} e^{\frac{j2\pi mk}{N}} & : k = n \\ \frac{1}{N} \sum_{m=0}^{L-1} \sum_{r=0}^{N-1} \Delta h_{r,m} e^{\frac{j2\pi r(n-k)}{N}} e^{-\frac{j2\pi nm}{N}} & : k \neq n \end{cases} \quad (7)
\end{aligned}$$

$[\alpha_0 \ \alpha_1 \ \dots \ \alpha_{L-1}]$ denote the average CIR and the CIR slope vectors of the OFDM block, respectively. The average CIR (or the middle row of \mathbf{H}) can be readily computed by performing an IFFT on the diagonal of \mathbf{G} , and then we are faced with the problem of estimating the CIR slope vector. The channel estimation algorithm proposed in [11] can be summarized as follows.

Step 1 Assume there are $P = \frac{N}{d}$ pilot subcarriers equally spaced at subcarriers $p(0), \dots, p(P-1)$ with a distance of d , i.e. $p(i) = i \times d$. Ignoring ICI, the frequency response at pilot subcarriers is

$$\hat{G}_{p(i),p(i)} = \frac{Y_{p(i)}}{X_{p(i)}} \quad : 0 \leq i \leq P-1 \quad (10)$$

Denoting the estimated frequency response by a length- P vector $\hat{\mathbf{g}}$, we estimate the entire main diagonal of \mathbf{G} by performing a linear or Wiener interpolation on $\hat{\mathbf{g}}$, followed by a P -point IFFT to estimate the average CIR, denoted by $\hat{\mathbf{h}}_{t-1}^{\text{avg}}$, where we assume that the current OFDM block index is $t-1$.

Step 2 Repeat Step 1 for the next two OFDM blocks so that we have the middle rows of \mathbf{H} for three consecutive OFDM blocks, denoted by $\hat{\mathbf{h}}_{t-1}^{\text{avg}}$, $\hat{\mathbf{h}}_t^{\text{avg}}$ and $\hat{\mathbf{h}}_{t+1}^{\text{avg}}$.

Step 3 For the t -th OFDM block, we denote by $\hat{\alpha}_1$ and $\hat{\alpha}_2$ the estimated CIR slope vectors for the first and second halves of the OFDM block, respectively, where the symbol index t is made implicit to simplify notation. Hence

$$\hat{\alpha}_1 = (\hat{\mathbf{h}}_t^{\text{avg}} - \hat{\mathbf{h}}_{t-1}^{\text{avg}})/N; \quad \hat{\alpha}_2 = (\hat{\mathbf{h}}_{t+1}^{\text{avg}} - \hat{\mathbf{h}}_t^{\text{avg}})/N \quad (11)$$

Step 4 Using the CIR slope vectors, we can compute the estimated off-diagonal elements of \mathbf{G} (see the Appendix for details). Combined with the estimated main diagonal obtained from Step 1, we now have an estimate of the full \mathbf{G} matrix which we denote by $\hat{\mathbf{G}}$.

To reduce the complexity of this hybrid channel estimation algorithm, we exploit the *sparseness* of time-domain CIR and the *banded* and *symmetric* structure of the frequency-domain channel matrix \mathbf{G} . In a typical SFN for the DVB environment, the CIR is sparse [12], i.e. it consists of a large number of zero or close-to-zero taps and these taps can be ignored to reduce the processing complexity with negligible performance loss. To exploit sparseness, we choose the M out of L taps from $\hat{\mathbf{h}}^{\text{avg}}$ with the largest absolute value, and zero out all the remaining taps. Therefore, we only need to estimate $M < L$ slopes when calculating $\hat{\alpha}_1$ and $\hat{\alpha}_2$ in (11). Choosing the value of M entails a complexity-performance tradeoff.

The banded structure of \mathbf{G} can also be exploited to reduce channel estimation complexity. Simulation results in Subsection VI-A show that a 3-tap FEQ [8] performs well for DVB-H (even at a relatively high Doppler of 10% for the 8K mode) which requires an estimate of only the three main diagonals of \mathbf{G} . Since the main diagonal of \mathbf{G} is estimated

in Step 1, we only need to compute one sub-diagonal and one super-diagonal of $\hat{\mathbf{G}}$ in Step 4 instead of the full matrix. Furthermore, since the elements of the sub-diagonals of \mathbf{G} are approximately the negatives of the corresponding elements of the super-diagonals for large N (see the Appendix for a proof), we only need to compute one super-diagonal of $\hat{\mathbf{G}}$.

C. ICI-Mitigating Pilot/Data Placement Scheme

Here, we propose a pilot/data placement scheme to mitigate ICI (and hence enhance the accuracy of estimating the main diagonal of \mathbf{G}) at pilot subcarriers by exploiting the fact that the sub-diagonals and super-diagonals of \mathbf{G} are approximately negatives of each other as shown in the Appendix.

We assume that the channel frequency response is fixed over $2i$ contiguous subcarriers (i.e. $G_{k,n} = G_{k-2i,n-2i}$). This is equivalent to assuming that the channel coherence bandwidth is significantly larger than the width of $2i$ subcarriers. For the TU06 channel model we use in this paper for the DVB environment, the channel coherence bandwidth is around 200 KHz while the subcarrier width is 4 KHz, 2 KHz or 1 KHz for the 2K, 4K and 8K modes, respectively. Hence, the channel can be assumed fixed over 4 adjacent subcarriers. Considering the $(n-1)$ element on the first super-diagonal, and using (15), we have $G_{n-1,n} \approx -G_{n+1,n} \approx -G_{n-1,n-2}$. Alternatively, we can write $G_{n,n+1} \approx -G_{n,n-1}$ which shows that the two adjacent ICI coefficients in (3) are approximately negatives of each other. Noting that the nearest two interference terms contribute the most to the ICI term in (3), we propose a pilot/data placement scheme to suppress ICI at pilot subcarriers by placing two identical data symbols on both sides of the pilot subcarrier. For example, we place the same data symbol $X_{p(i)-1}$ on the $p(i)-1$ and $p(i)+1$ subcarriers where $p(i)$ is a pilot index. Equation (3) can be rewritten as

$$\begin{aligned}
Y_{p(i)} &= G_{p(i),p(i)} X_p + (G_{p(i),p(i)-1} + G_{p(i),p(i)+1}) X_{p(i)-1} \\
&\quad + \sum_{\substack{n=0 \\ n \neq p(i)-1, p(i), p(i)+1}}^{N-1} G_{p(i),n} X_n + V_{p(i)}
\end{aligned}$$

It is clear that the second term on the right-hand side of the above equation is approximately zero, and this will reduce the ICI term at the i -th pilot subcarrier significantly which will improve channel estimation accuracy for the main diagonal of \mathbf{G} in Step 1 of Subsection III-B.

IV. DIFFERENTIAL ICI CANCELLATION

To further reduce the receiver cost by eliminating the complexity of channel estimation, we investigate non-coherent OFDM detection with a focus on differential schemes due

to their implementation simplicity. We first present the basic principles of differential detection and then describe an ICI cancellation scheme compatible with differential detection.

A. Differential OFDM

In OFDM systems, differential encoding can be implemented either across subcarriers (frequency-domain) or across OFDM blocks (time-domain). We found that frequency-domain differential encoding is a better choice for DVB-H systems under high-mobility, and the reason will become apparent soon.

Let $[U_1 \dots U_{N-1}]^T$ and $[X_1 \dots X_{N-1}]^T$ denote the information-bearing and the transmitted OFDM blocks, respectively. For the k -th subcarrier, the differential encoding rule is $X_k = X_{k-1}U_k$. Ignoring ICI and noise, we write the input/output relations for subcarriers k and $k-1$ as

$$Y_{k-1} = G_{k-1,k-1}X_{k-1}; Y_k = G_{k,k}X_k \quad (12)$$

Assuming the channel fixed over two adjacent subcarriers, i.e. $G_{k,k} = G_{k-1,k-1}$ and using (12), we have $U_k = Y_k/Y_{k-1}$. The assumption that the channel is fixed over 2 adjacent subcarriers is accurate (see discussion in Section III-C). Time-domain differential encoding, on the other hand, requires a fixed channel over 2 adjacent OFDM blocks, i.e. the channel coherence time is much larger than the duration of 2 OFDM blocks. Since this assumption is not valid under the high-Doppler DVB-H scenarios considered in this paper, we adopt differential encoding across subcarriers. Our simulation results in Section VI show that differential OFDM is robust to modest Doppler; however, an error floor is still observed under high Doppler. To further improve the performance, we briefly discuss in the following subsection an ICI-mitigating scheme which does not require channel information at the receiver and hence is compatible with differential detection.

B. ICI Self-Cancellation Scheme for Differential OFDM

ICI self-cancellation is a simple yet effective method proposed by Zhao [13] to combat ICI which uses a repetition code particularly designed to minimize ICI at the cost of spectral efficiency. The ICI self-cancellation scheme does not require channel information at the receiver and enjoys low implementation complexity. However, since each data symbol is modulated twice, the bandwidth efficiency will be reduced by a half. This can be compensated for by using a higher-order signal constellation or a rate-2 two-transmit-antenna scheme such as spatial multiplexing.

V. COMPLEXITY ANALYSIS

Steps 1-3 of the hybrid channel estimation algorithm in Section III-B have significantly less complexity than Step 4. To see this, we note that Step 1 mainly involves a P -point FFT and assuming a radix-2 FFT, this operation requires $(P/2)\log_2(P)$ complex multiplications. Step 2 requires no additional computations since for each OFDM block, $\hat{\mathbf{h}}^{avg}$ needs to be computed only once and Step 3 requires $2L$ divisions. The complexities for these three steps are negligible compared to that of Step 4; hence, we only consider the complexity of Step 4.

TABLE I
COMPLEXITY REDUCTIONS FOR THE HYBRID CHANNEL ESTIMATION ALGORITHM

Mode (N)	# of multiplications ($N_{multi.}$)		
	2K	4K	8K
M=10, D=1	13850	27776	55628
M=10, D=2	15898	31872	62820
M=10, D=N-1	6.2×10^6	2.5×10^7	1.0×10^8
M=64, D=1	20253	40832	81792
M=64, D=2	22400	44928	89984
M=64, D=N-1	6.2×10^6	2.5×10^7	1.0×10^8

In Step 4, to compute the off-diagonal elements of \mathbf{G} using Equation (17) in the Appendix, we first need to calculate the two numerators, each of which is an N -point IFFT of a size- L vector (namely $\hat{\alpha}_1 + \hat{\alpha}_2$ and $\hat{\alpha}_1 - \hat{\alpha}_2$), which has a complexity of $[\log_2 L + 2(1 - \frac{L}{N})] \cdot \frac{N}{2}$ complex multiplications [14]. In [15], a generic FFT pruning algorithm is proposed which does not require the sparse input data to be grouped together (as in our case where the M active taps are dispersed among all L CIR taps). This algorithm gives a complexity saving ratio of β ; hence, we need approximately $(1 - \beta)[\log_2 L + 2(1 - \frac{L}{N})]N$ complex multiplications for 2 IFFT operations in the numerator, where β is given in [15] for different scenarios. The denominators in (17) are all fixed; hence, their reciprocals can be computed offline and stored. Therefore, to compute one off-diagonal element $G_{n+i,n}$ according to (17), we need two complex multiplications for odd-indexed diagonals and one for even-indexed diagonals¹. Our reduced-complexity approach exploits the symmetry of \mathbf{G} and computes only D subdiagonals for a Q -tap FEQ ($Q = 2D + 1$), which requires $(3\lfloor \frac{D}{2} \rfloor + 2(D)_2)N$ complex multiplications. Denoting the total number of multiplications by $N_{multi.}$, we have

$$N_{multi.} = (1 - \beta)(\log_2 L + 2(1 - \frac{L}{N}))N + (3\lfloor \frac{D}{2} \rfloor + 2(D)_2)N \quad (13)$$

Table I lists the total number of multiplications required by the hybrid channel estimation algorithm assuming an $L = 64$ tap CIR for different M , D and N . Exploiting CIR sparseness by using $M = 10$ instead of 64 taps, the IFFT complexity is reduced by approximately 40% (i.e. $\beta \approx 0.4$) [15]. In addition, by exploiting the banded structure of \mathbf{G} (i.e. assuming a tri-diagonal \mathbf{G} with $D = 1$ instead of a full \mathbf{G} with $D = N - 1$), the number of required multiplications is reduced by 99.97%. These significant reductions in the number of complex multiplications can be seen from the second term on the right-hand side of (13), which has $\mathcal{O}(N)$ complex multiplications (assuming $D \ll N$), while it is $\mathcal{O}(N^2)$ for a full-matrix estimate of \mathbf{G} .

To detect one OFDM block, the Q -tap FIR-MMSE FEQ in [8] requires N Q -by- Q matrix inversions and NQ complex multiplies, for a total of $NQ(Q+1)$ multiplies. As a numerical example, consider the scenario $D = 1$, $Q = 2D + 1 = 3$, $N = 8192$, $M = 10$, $L = 64$ and an 8K mode DVB-H block duration of $952\mu\text{sec}$. Furthermore, we make the simple assumption that each complex multiplication can be performed in one instruction. Then, the hybrid channel estima-

¹Here, a diagonal means a cyclicly-shifted diagonal with N elements.

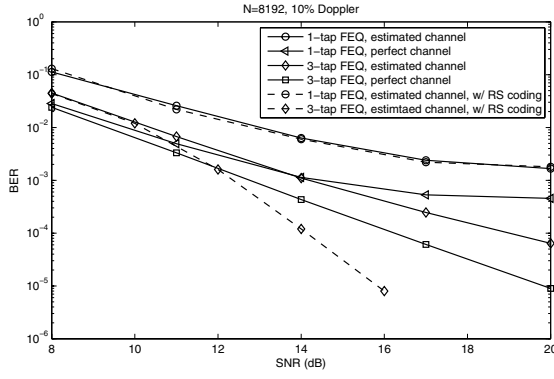


Fig. 1. BER performance of hybrid frequency/time-domain channel estimation algorithm with 1 and 3-tap FEQ (8K mode, 10% Doppler)

tion algorithm requires 55,628 instructions per OFDM block while the 3-tap FIR-MMSE FEQ coefficient computation and application to data requires 98,304 instructions per OFDM block for a total of 153,932 instructions per OFDM block or equivalently 162 Million Instructions Per Second (MIPS), which is well within the processing power of state-of-the-art programmable DSP chips.

VI. SIMULATION RESULTS

We evaluated the DVB-H receiver performance mostly in the 8K mode with $N = 8192$ since this mode suffers more from ICI than the 2K or 4K modes. We assumed the typical urban TU-06 channel delay profile defined by the COST 207 project with 6 taps in the continuous-time domain [16], 8 MHz channel bandwidth, and a carrier frequency of 800 MHz. The TU-06 model was shown to give an accurate description of the DVB mobile radio channel [17]. The CIR delay spread is 5 μ sec and after sampling, we have a long discrete-time CIR with approximately 64 taps. Each discrete channel tap is generated by an independent complex Gaussian random variable with time correlation based on Jake's model. A 64-state rate-1/2 convolutional code with octal generator (133,171) is employed. The coded bits are interleaved within an OFDM block and mapped into QPSK symbols which are transmitted in blocks each appended with a CP longer than the channel memory. We inserted scattered pilots separated by 12 data subcarriers ($d = 12$), as in the DVB-H standard, and we assumed that all N subcarriers are active.

A. Coherent OFDM Detection Results

The performance of the 8K mode is evaluated with a Doppler of 10% corresponding to a highway speed of approximately 100 Km/h in this simulation, and the result is shown in Fig. 1. Since there is significant ICI due to high Doppler, error floors are observed for both estimated and perfect channel scenarios with 1-tap FEQ. To combat ICI, we implemented the hybrid frequency/time-domain channel estimation algorithm in Subsection III-B to estimate the 3 main diagonals of \mathbf{G} and implemented a 3-tap FEQ which eliminates the error floor. Also shown in this figure is the additional performance improvement achieved when concatenating an outer Reed-Solomon (RS) code with octal generator (204,188) [7]. It can

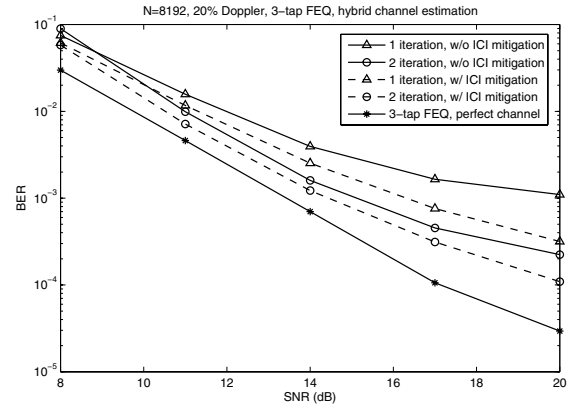


Fig. 2. BER performance of reduced-complexity hybrid frequency/time-domain channel estimation algorithm with ICI mitigating pilot/data placement scheme and joint channel/data estimation (8K mode, 20% Doppler)

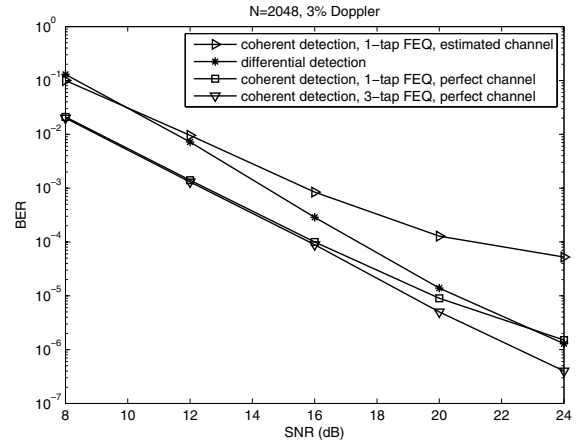


Fig. 3. BER comparison between coherent vs. differential OFDM (2K mode, 3% Doppler)

be seen that RS coding hardly gives any improvement for the 1-tap FEQ scenario where the number of errors exceeds the error correction capability of the used RS code, while it significantly improves the performance of a 3-tap FEQ with estimated channel.

The Doppler frequency can be as high as 20% if the receiver is moving at fast train speeds or if the DVB system is operating on an L-band channel with approximately 1.6 GHz carrier frequency. To handle the severe ICI due to this extremely high Doppler, we implemented the ICI-mitigating pilot/data placement scheme in Subsection III-C and integrated it with a joint channel estimation and data detection scheme where we use the hard-decision-detected data from the previous iteration as pilots. Fig. 2 shows that the second iteration with a pilot spacing of $d' = 4$ subcarriers significantly improves performance compared to the first iteration. It can also be observed that the ICI-mitigating pilot/data placement scheme further improves the performance by approximately 2 dB for the second iteration.

B. Differential OFDM Detection Results

Fig. 3 compares coherent and differential detection for the DVB-H 2K mode with a normalized Doppler of 3% which

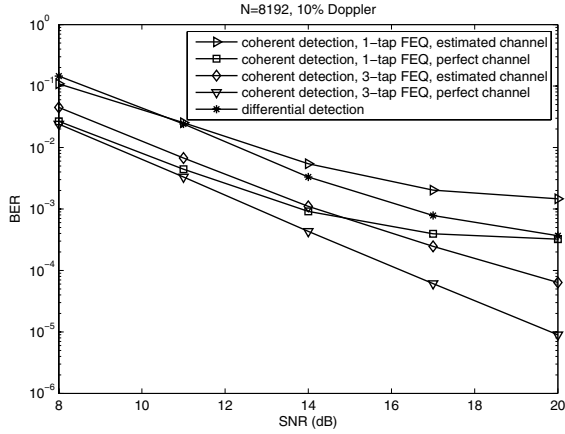


Fig. 4. BER comparison between coherent and differential OFDM (8K mode, 10% Doppler)

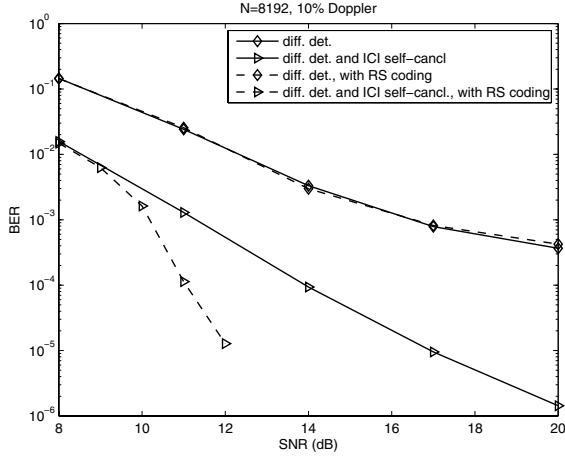


Fig. 5. BER performance of differential schemes with RS coding (8K mode, 10% Doppler)

corresponds to a highway speed of approximately 110 Km/h in this simulation. It can be seen that differential OFDM detection outperforms coherent detection with an estimated channel and 1-tap FEQ, and is comparable to it with a perfect 1-tap FEQ at high SNR. The 8K mode suffers more from ICI since the subcarrier spacing is reduced by a factor of 4 compared to the 2K mode. The performance comparison for the 8K mode is evaluated at a higher Doppler of 10% corresponding also to a highway speed, and the result is depicted in Fig. 4. Since there is much more significant ICI in the 8K mode, error floors are observed for both 1-tap FEQ coherent detection (estimated or perfect channel) and differential detection. The error floor is eliminated (for the considered SNR range) with a 3-tap FEQ even with estimated channel information.

Finally, Fig. 5 presents the performance of differential OFDM detection with RS coding under 10% Doppler for 8K mode. We observe that RS coding hardly gives any performance improvement with differential transmission only. However, when it is integrated with the ICI self-cancellation scheme, it becomes much more effective. Hence, it is necessary to combine differential OFDM detection with more

advanced ICI mitigation techniques at high Doppler.

VII. CONCLUSIONS

Utilizing the sparse nature of the time-domain CIR and the banded and symmetric structure of the frequency-domain channel matrix in DVB-H, we developed a reduced-complexity hybrid frequency/time-domain channel estimation algorithm which improves performance significantly under high Doppler with substantial complexity reductions. To further suppress ICI, we integrated this channel estimation algorithm with an ICI-mitigating pilot/data placement and joint channel/data detection schemes, and demonstrated further appreciable performance improvements even at a very high Doppler of 20%.

In addition, we investigated differential transmission as a low-complexity ICI-resilient option for the DVB-H system. Since differential OFDM detection does not require channel estimation, it can eliminate not only the channel estimation pilot overhead of the DVB-H system but also its implementation complexity at the receiver as well. While we consider DVB-H as an application, the techniques presented in this paper can be applied to other mobile OFDM systems such as WiMAX.

APPENDIX

Substituting for the (k, n) entry index of \mathbf{G} in (7) with $(n + i, n)$ and combining it with (6), the n -th element of the i -th sub-diagonal ($i \neq 0$) is given by

$$\begin{aligned} G_{n+i,n} &= \frac{1}{N} \sum_{m=0}^{L-1} \sum_{r=0}^{N-1} \left(r - \frac{N-1}{2}\right) \alpha_m e^{\frac{j2\pi r(-i)}{N}} e^{-\frac{j2\pi n m}{N}} \\ &= -\frac{\sum_{m=0}^{L-1} \alpha_m e^{-\frac{j2\pi n m}{N}}}{1 - e^{\frac{j2\pi(-i)}{N}}} = -\frac{\sum_{m=0}^{L-1} \alpha_m e^{-\frac{j2\pi n m}{N}}}{j\theta} \end{aligned} \quad (14)$$

where for large N , we defined $\theta = \frac{2\pi(-i)}{N} \approx 0$. Similarly, the element on the i -th super-diagonal and the n -th column is

$$G_{n-i,n} \approx -\frac{\sum_{m=0}^{L-1} \alpha_m e^{-\frac{j2\pi n m}{N}}}{j(-\theta)} \approx -G_{n+i,n} \quad (15)$$

Therefore, two elements on the same column of the sub and super-diagonal are approximately negatives of each other for a large FFT size as in the DVB-H system. Using two slopes as in Step 4 of the channel estimation algorithms in Subsection III-B requires a minor change in (6), which can be rewritten as

$$\Delta h_{r,m} = \begin{cases} \left(r - \frac{N-1}{2}\right) \alpha_{1,m} & : 0 \leq r < N/2 \\ \left(r - \frac{N-1}{2}\right) \alpha_{2,m} & : N/2 \leq r \leq N-1 \end{cases} \quad (16)$$

and in this case $G_{n+i,n}$ is given by (17) shown on top of this page.

Equation (17) shows that even-indexed diagonals have the same expression as in the single-slope case given in (15). Hence, the elements of the super-diagonals are negatives of those on the sub-diagonals. The expression for the odd-indexed diagonals case, on the other hand, has an extra term. However, our DVB-H simulations show that in most cases,

$$G_{n+i,n} = \begin{cases} -\frac{\sum_{m=0}^{L-1} (\alpha_{1,m} + \alpha_{2,m}) e^{-\frac{j2\pi nm}{N}}}{2 \times (1 - e^{\frac{j2\pi(-i)}{N}})} + \frac{\sum_{m=0}^{L-1} 2(\alpha_{1,m} - \alpha_{2,m}) e^{-\frac{j2\pi nm}{N}}}{N \times (1 - e^{\frac{j2\pi(-i)}{N}})^2} & : i = 1, 3 \dots \\ -\frac{\sum_{m=0}^{L-1} (\alpha_{1,m} + \alpha_{2,m}) e^{-\frac{j2\pi nm}{N}}}{2 \times (1 - e^{\frac{j2\pi(-i)}{N}})} & : i = 2, 4 \dots \end{cases} \quad (17)$$

the CIR slope almost remains constant across two OFDM blocks, i.e. $\alpha_{1,m} \approx \alpha_{2,m}$, and consequently (17) reduces to (14). Hence, the same conclusion is approximately valid for the case of odd-indexed diagonals.

REFERENCES

- [1] G. Faria, J. Henriksson, E. Stare, and P. Talmola, "DVB-H: digital broadcast services to handheld devices," *Proceedings of IEEE*, vol. 94, pp. 194–209, Jan 2006.
- [2] S. Kim and G. Pottie, "Robust OFDM in fast fading channel," in *Proceedings of GLOBECOM*, vol. 2, Dec 2003, pp. 1074–1078.
- [3] W. Jeon, K. Chang, and Y. Cho, "An equalization technique for orthogonal frequency-division multiplexing systems in time-variant multipath channels," *IEEE Trans. Commun.*, vol. 47, pp. 27–32, Jan 1999.
- [4] Y. Choi, P. Voltz, and F. Cassara, "On channel estimation and detection for multicarrier signals in fast and selective Rayleigh fading channels," *IEEE Trans. Commun.*, vol. 49, pp. 1375–1387, Aug 2001.
- [5] T. Cui, C. Tellambura, and Y. Wu, "Low-complexity pilot-aided channel estimation for OFDM systems over doubly-selective channels," in *Proc. of IEEE International Conference on Communication*, vol. 3, May 2005, pp. 1980 – 1984.
- [6] A. Stamoulis, S. Diggavi, and N. Al-Dhahir, "Intercarrier interference in MIMO OFDM," *IEEE Trans. Signal Process.*, vol. 50, pp. 2451–2464, Oct 2002.
- [7] ETSI EN 300 744 V1.5.1, "Digital Video Broadcasting (DVB): Framing structure, channel coding and modulation for digital terrestrial television," *ETSI*, 2004.
- [8] S. Lu, R. Kalbasi, and N. Al-Dhahir, "OFDM interference mitigation algorithms for doubly-selective channels," in *Proc. of IEEE Vehicular Technology Conference*, Sep 2006, pp. 1–5.
- [9] X. Cai and G. Giannakis, "Bounding performance and suppressing inter-carrier interference in wireless mobile OFDM," *IEEE Trans. Commun.*, vol. 51, pp. 2047–2056, Dec 2003.
- [10] L. Rugini, P. Banelli, and G. Leus, "Low-complexity banded equalizers for OFDM systems in doppler spread channels," *EURASIP Journal on Applied Signal Processing*, Jan 2007.
- [11] Y. Mostofi and D. Cox, "ICI mitigation for pilot-aided OFDM mobile systems," *IEEE Trans. Wireless Commun.*, vol. 4, pp. 765–774, Mar 2005.
- [12] C. Carbonelli, S. Vedantam, and U. Mitra, "Sparse channel estimation with zero tap detection," *IEEE Trans. Wireless Commun.*, vol. 6, pp. 1743–1763, May 2007.
- [13] Y. Zhao and S.-G. Haggman, "Intercarrier interference self-cancellation scheme for OFDM mobile communication systems," *IEEE Trans. Commun.*, vol. 49, pp. 1185–1191, Jul 2001.
- [14] J. Markel, "FFT pruning," *IEEE Trans. Audio Electroacoust.*, vol. 19, pp. 305–311, Dec 1971.
- [15] Z. Hu and H. Wan, "A novel generic fast Fourier transform pruning technique and complexity analysis," *IEEE Trans. Signal Process.*, vol. 53, pp. 274–282, Jan 2005.
- [16] "COST 207: Digital land mobile radio communications, Euro. Project Final Rep. EUR 12 160," 1998.
- [17] S. Tomasin, A. Gorokhov, H. Yang, and J. Linnartz, "Iterative interference cancellation and channel estimation for mobile OFDM," *IEEE Trans. Wireless Commun.*, vol. 4, pp. 238–245, Jan 2005.